

THIRTEENTH EUROPEAN ROTORCRAFT FORUM

Paper No. ⁷⁷93

AN INVESTIGATION OF THE STABILITY OF FLIGHT PATH CONSTRAINED
HELICOPTER MANOEUVRES BY INVERSE SIMULATION

D.G. Thomson

R. Bradley

September 8-11, 1987

ARLES, FRANCE

ASSOCIATION AERONAUTIQUE ET ASTRONAUTIQUE DE FRANCE

AN INVESTIGATION OF THE STABILITY OF FLIGHT PATH CONSTRAINED
HELICOPTER MANOEUVRES BY INVERSE SIMULATION.

D.G. Thomson and R. Bradley

Dept. of Aeronautics and Fluid Mechanics
University of Glasgow.

Summary

Inverse solution of the helicopter equations of motion involves the calculation of the control sequences required to fly a defined manoeuvre. A package capable of performing such solutions has been developed and is briefly described in this paper. These inverse solutions have given some insight into potential stability problems associated with constrained flight, and a technique for predicting these instabilities has been developed.

Nomenclature

A	System matrix of helicopter
A_C	Modified system matrix
B	Control matrix of helicopter
B_C	Input matrix for inverse solution
h	Altitude
p, q, r	Roll, pitch and yaw rates
t_m	Manoeuvre time
u, v, w	Translational velocities in body axes
u_0, v_0, w_0	Reference values of translational velocities
$\dot{u}, \dot{v}, \dot{w}$	Translational accelerations in body axes
\underline{u}	Control vector
$\dot{x}, \dot{y}, \dot{z}$	Translational velocities in earth axes
$\ddot{x}, \ddot{y}, \ddot{z}$	Translational accelerations in earth axes
\underline{x}	State vector
θ, ϕ, ψ	Pitch, roll and yaw attitude angles
θ_0	Main rotor collective pitch angle
θ_{otr}	Tail " " " " " " " " " "
θ_{1c}	" " " " lateral cyclic pitch angle
θ_{1s}	" " " " longitudinal " " " " " " "

1. Introduction

The ability to perform flight path constrained manoeuvres is a requirement of almost all aircraft. The manoeuvres may be common, such as approach and landing, or more specialised as, for example, in maritime surveillance or aerial combat. Traditionally it is the task of the pilot to control the execution of these manoeuvres but there is an increasing application of automatic techniques. This current interest in flight path

constrained manoeuvres has provided the motivation for the development of methods for solving the inverse problem of aircraft motion, that is, given a specified flight path where the aircraft's position is a known function of time, find the control movements which are necessary to fly that path.

Helicopters flying in a nap-of-the-earth (NOE) environment are required to perform well defined manoeuvres associated with concealment, obstacle avoidance and weapons delivery (Ref. 1). A method has been developed which solves directly the inverse problem for helicopters flying these classes of manoeuvre (Refs. 2, 3). This inverse method has been incorporated in a computer package designated HELINV. Initially, this package was developed for use in evaluation of helicopter agility (Refs. 3, 4) but has also provided insight into the potential problems of instability which can result from a constrained flight path.

2. A Description of the Inverse Method

A comprehensive description of the inverse method used in HELINV is given in Reference 3. A brief outline is included here dealing with the main aspects of the inverse simulation : the mathematical model, the inputs to the model, and the solution algorithm.

2.1 The Mathematical Model

Previous methods of solving the inverse problem have relied on reduced order or full linear models (Ref. 5). The use of a linearised model limits the severity of manoeuvre over which valid inverse solutions can be obtained. The approach taken at Glasgow University does not require any compromise on the quality of the mathematical model, and uses the model which is incorporated in the HELISTAB simulation package (Ref.6) developed by the Flight Systems Division of the Royal Aircraft Establishment. This model is nonlinear, has six degrees of freedom and is of proven validity over a wide range of flight conditions. Using the HELISTAB model allows valid inverse solutions to be found for various configurations flying a wide range of manoeuvres.

2.2 Definition of Manoeuvres

In an inverse simulation the inputs into the system are the required manoeuvres. A series of NOE manoeuvres (such as pop-ups, turns, accelerations etc.) are available in the HELINV package. Manoeuvres are defined by specifying the helicopter's flight velocity, V , position (x,y,z) , and angle of sideslip, β , as functions of time. A flight path in three dimensions is defined by specifying the helicopter's position in the xy plane as a function of time, then defining altitude changes around the resulting track. Flight speed and sideslip are both constrained either to be constant, or vary as a polynomial function of time. For example, the hurdle-hop manoeuvre shown in Figure 1 is defined by specifying altitude, z , as a function of time, the track simply being the x -axis. All manoeuvres in the HELINV package begin and end at a defined trim state therefore the flight path specifying function must satisfy the boundary conditions

- 1) $t = 0, \quad z = 0, \quad \dot{z} = 0, \quad \ddot{z} = 0$
- 2) $t = t_m/2, \quad z = -h, \quad \dot{z} = 0$
- 3) $t = t_m, \quad z = 0, \quad \dot{z} = 0, \quad \ddot{z} = 0.$

A simple analytic function which fulfills these conditions is a seventh order polynomial. The user then simply specifies the desired hurdle height, h , and total distance, s , and an iterative solution is used to find the manoeuvre time t_m , and hence the coefficients of the polynomial. The helicopter's (x,y,z) components of earth axis acceleration and velocity can then be found directly. It is worth emphasizing that these manoeuvres are defined independently of any helicopter model or configuration, and indeed may not be flyable by the helicopter being simulated.

2.3 The Inverse Algorithm

The manoeuvre is divided into a series of equally spaced time points, the equations of motion are then solved at each of them to give the control time histories needed to fly this manoeuvre. The equations are solved using an iterative scheme with the attitude angles θ, ϕ as the unknowns. At each time point, the solution is started by making an initial guess of the values of these angles. It is then possible (knowing the value of sideslip velocity, v , from the specified sideslip angle and flight velocity) to calculate the corresponding value of the third attitude angle, ψ . The body fixed axes velocities and accelerations can then be found by using an Euler angle transformation. Next the rotational velocities and accelerations are calculated using numerical differentiation of the attitude angles. With all of the state variables available it is possible to evaluate all of the fuselage aerodynamic forces and moments, and the equations of motion may be used to solve for the correct θ and ϕ using the Newton Raphson procedure. Coincidentally the main and tail rotor forces and moments are determined, from which the control angles are calculated. Rather than seek a global solution, the equations of motion are solved progressively through the manoeuvre. This economic structuring of the algorithm allows rapid solution which is important in making the inverse method a practical tool. The implicit nature of the algorithm is conducive to numerical stability.

3. Examples of Inverse Solutions

The most useful feature of an inverse method is that a series of helicopter configurations can be simulated flying a single precisely defined manoeuvre. The required control and resulting attitude responses can then be compared, highlighting the merits and deficiencies of the various configurations. To illustrate this facility, inverse solutions have been found for a hurdle-hop manoeuvre flown by two versions of a conventional battlefield helicopter of mass of 4500 kg and having four blades of radius 6.5m. One of the two variants has a flapwise stiff, Semi-Rigid Rotor (configuration SRR), the other a fully Articulated Rotor (configuration AR). In the HELISTAB model, blade flapping is simulated by using a centre spring equivalent rotor with a flapping stiffness spring constant, K_β . The value of K_β is chosen to give the same rotating and non-rotating flapping frequencies as those of the true blade. In this paper the flapping stiffness of the SRR and AR helicopters have been given

typical values 170 and 50 kNm/rad respectively. All other rotor and fuselage parameters are the same for both configurations.

3.1 Results for a HURDLE-HOP Manoeuvre

The attitude and control time histories for both aircraft flying a hurdle-hop manoeuvre are given, plotted as displacements from a trim condition, in Figure 2. The hurdle height, h , is 25m, the total distance, s , is 500m, angle of sideslip is constrained to be zero and the whole manoeuvre is flown at a constant velocity of 80 knots.

The rotors of both helicopter's will produce approximately the same thrust in a given flight condition since they both have the same aerodynamic properties. Any small difference between the thrusts will be due to slightly different flapping angles. This explains why the time histories of main rotor collective, θ_0 , are identical. As both vehicles are similar, the total rotor moment required to perform the manoeuvre will be similar. This moment is composed of a contribution due to the elastic stiffness of the rotor (governed by K_β) and a contribution due to the offset of the thrust vector from the helicopter centre of gravity (caused by rotor disc tilt). Since the SRR configuration has a much higher K_β , the disc tilt required to produce a given rotor moment is less. This is evident by the smaller displacements in the longitudinal (θ_{1S}) and lateral (θ_{1C}) cyclic pitch angles of the SRR configuration. The smaller disc tilt of the SRR helicopter also produces smaller excursions in pitch attitude, θ . The higher degree of coupling between longitudinal and lateral dynamics associated with rigid rotor helicopters is illustrated by the plots of roll angle, ϕ .

This example gives an insight into the power of inverse methods to give directly comparable information about different configurations. The results appear to be correct in size and trend, however some form of validation is obviously necessary.

3.2 Validation of Results

In the context of an inverse method using an established mathematical model (HELISTAB), the validation stage is strictly to confirm the consistency of the results between HELINV and HELISTAB. Verification of results is therefore achieved by performing a conventional time response calculation using the control time histories generated by HELINV as inputs to the HELISTAB mathematical model. The resulting "control generated" flight path can then be compared with the "commanded" flight path.

The control time histories of the AR helicopter flying the hurdle-hop manoeuvre have been used to perform a time response solution, from which a control generated flight path has been computed. This is compared with the commanded path in Figure 3. There is little difference between the two paths : a small discrepancy at the exit is visible on the altitude plot, and a maximum drift of about 0.06m over the 500m track. The discrepancies are entirely consistent with the different numerical integration methods used in the forward and inverse solutions. A result of similar quality is obtained using the control time histories of the SRR helicopter.

3.3 Oscillatory Solutions

Not all solutions found by HELINV are as well defined or easily explained as those for the hurdle-hop described above. When a small calculation time step is used, oscillations often begin to appear in the solution. As the time step is reduced the amplitude of these oscillations increases, their period remaining constant. These oscillations can be observed in the following example of the simulation of turning flight. Turning manoeuvres are specified by defining turn rate as a function of time. This allows continuity where linear sections of track join curved sections. In this example turn rate is defined, as shown in Figure 4, as having a constant value over the main section of the manoeuvre (giving a circular track) with cubic polynomial functions of time to define the entry and exit transients. The flight path co-ordinates at the exit are supplied (in terms of an effective radius) and an iterative sequence is used to find an appropriate value of maximum, steady turn rate, \dot{x}_m . The control and attitude time histories for the SRR helicopter flying this type of turn, of effective radius 200m, at constant height and velocity of 80 knots is given in Figure 5. The calculation time step is 0.08 seconds.

Again, the plots appear, intuitively, to be correct both in size and trend. As the middle section of the manoeuvre is a steady turn, all variables would be expected to reach a certain steady value, then remain constant until the exit transient. However, it is noticeable, especially in the plots of fuselage attitude, θ , and longitudinal cyclic, θ_{1s} , that there is a damped oscillation about this steady value. Despite the oscillations, valid solutions are still being found, as can be observed in the comparison of control generated and commanded flight paths shown in Figure 6. The oscillations become more pronounced when the calculation is repeated with a smaller time step, as shown in Figure 7 where it was reduced to 0.02 seconds. There appear to be two distinct oscillations - one of period just over 1 second (visible in the plots of θ and θ_{1s}), and the other has a period of about 0.7 seconds (visible on all other plots). The dependence on the size of the time increment is suggestive of an inconsistency of the discrete formulation but its origin has a simpler explanation and is discussed in section 4.3 after some preliminary analysis.

To check whether the oscillations were simply due to the natural modes of the aircraft, a linearised version of the HELISTAB model was used to compute the helicopter's eigenvalues. Oscillatory modes of period 2.8 and 16.8 seconds were predicted for the SRR helicopter at a steady velocity of 80 knots. Neither of these modes match the oscillations visible in the inverse solution. The conclusion is that the constraint of flying a predetermined flight path is significantly modifying the dynamic characteristics of the system. An investigation to quantify this effect is a required adjunct to the inverse method.

4. A Linearised Representation of the Inverse Problem

A convenient way of analysing the stability of a nonlinear dynamic system is by linearising its equations of motion. The equations can be written in a convenient matrix form and simple matrix operations used to determine the dynamic characteristics of the system. For this reason it

would seem logical that a linearised statement of the inverse method will be of use in the investigation of the irregularities present in the HELINV solutions. For consistency, a linearised version of the HELISTAB mathematical model was used. The linearised helicopter equations of motion can be written in the form :

$$\dot{\underline{x}} = \underline{A} \underline{x} + \underline{B} \underline{u} \quad \dots (1)$$

where

$$\underline{x} = [u, v, w, p, q, r, \theta, \phi, \psi]^T,$$

$$\underline{u} = [\theta_0, \theta_{1s}, \theta_{1c}, \theta_{0tr}]^T,$$

\underline{A} = the system matrix,

\underline{B} = the control matrix.

The matrices, \underline{A} and \underline{B} , contain the aerodynamic derivatives and relevant gravitational and velocity terms. The linearised equations, when arranged in the form given by equation (1), can be used to describe the unconstrained motion of a helicopter in response to an applied series of control inputs. The eigenvalues of the helicopter are found from the system matrix, hence the period and damping of any oscillatory modes can be found.

The inverse solution of the nonlinear equations of motion is made unique by imposing four constraints on the helicopter's dynamics : the three accelerations in earth-axes (functions of the flight path geometry and the helicopter's speed), and sideslip velocity, are all given specified values. In effect, specifying the earth-axes accelerations, applies constraints to the body-axes accelerations. Specifying sideslip velocity leads, through yaw angle, ψ , to a constraint on yaw rate, r . The four principally constrained variables can be grouped together to form a vector \underline{x}_1 . Hence, if :

$$\underline{x}_1 = [u, v, w, r]^T \quad \text{and} \quad \underline{x}_2 = [p, q, \theta, \phi, \psi]^T,$$

then the system matrix of equation (1), when partitioned, becomes :

$$\begin{bmatrix} \dot{\underline{x}}_1 \\ \dot{\underline{x}}_2 \end{bmatrix} = \begin{bmatrix} \underline{A}_{11} & \underline{A}_{12} \\ \underline{A}_{21} & \underline{A}_{22} \end{bmatrix} \begin{bmatrix} \underline{x}_1 \\ \underline{x}_2 \end{bmatrix} + \begin{bmatrix} \underline{B}_1 \\ \underline{B}_2 \end{bmatrix} \underline{u} \quad \dots (2)$$

The vectors \underline{x}_1 and $\dot{\underline{x}}_1$ contain the specified values of the constraints and are therefore known at every point in the manoeuvre. The matrix equation (2) can be rewritten :

$$\dot{\underline{x}}_1 = \underline{A}_{11} \underline{x}_1 + \underline{A}_{12} \underline{x}_2 + \underline{B}_1 \underline{u} \quad \dots (3)$$

$$\dot{\underline{x}}_2 = \underline{A}_{21} \underline{x}_1 + \underline{A}_{22} \underline{x}_2 + \underline{B}_2 \underline{u} \quad \dots (4)$$

From equation (3) :

$$\underline{u} = \mathbf{B}_1^{-1} [\dot{\underline{x}}_1 - \mathbf{A}_{11} \underline{x}_1 - \mathbf{A}_{12} \underline{x}_2]$$

Substituting this into equation (4) gives, with manipulation :

$$\dot{\underline{x}}_2 = [\mathbf{A}_{22} - \mathbf{B}_2 \mathbf{B}_1^{-1} \mathbf{A}_{12}] \underline{x}_2 + [(\mathbf{A}_{21} - \mathbf{B}_2 \mathbf{B}_1^{-1} \mathbf{A}_{11}) \dot{\underline{x}}_1 + (\mathbf{B}_2 \mathbf{B}_1^{-1}) \underline{x}_1]$$

Hence, if :

$$\left. \begin{aligned} \mathbf{A}_C &= \mathbf{A}_{22} - (\mathbf{B}_2 \mathbf{B}_1^{-1}) \mathbf{A}_{12} \\ \mathbf{B}_C &= [(\mathbf{A}_{21} - (\mathbf{B}_2 \mathbf{B}_1^{-1}) \mathbf{A}_{11}) \quad (\mathbf{B}_2 \mathbf{B}_1^{-1})] \\ \underline{u}_C &= \begin{bmatrix} \dot{\underline{x}}_1 \\ \underline{x}_1 \end{bmatrix} \end{aligned} \right\} \dots (5)$$

then the constrained system is represented by :

$$\dot{\underline{x}}_2 = \mathbf{A}_C \underline{x}_2 + \mathbf{B}_C \underline{u}_C \quad \dots (6)$$

\mathbf{A}_C and \mathbf{B}_C can be considered as the system and control matrices of the constrained helicopter. Since it contains the constraint vectors, \underline{u}_C is equivalent to a control vector in an inverse solution, the constraints, in effect, being the inputs to the system. The only limitation on the use of this analysis is that the matrix, \mathbf{B}_1 , must be nonsingular.

4.1 Calculation of Constrained System and Control Matrices

The first stage in the calculation of the new system and control matrices must be to replace the constrained variables (u,v,w,r) by their specifying functions.

a) Body-axes Velocities and Accelerations

The helicopter's body-axes velocities and accelerations are found using the Euler transformations, the velocities and accelerations in the earth-axes system being specified as functions of time. By linearising the transformation equation the perturbed body-axes velocities are given by :

$$\begin{bmatrix} u \\ v \\ w \end{bmatrix} = \begin{bmatrix} l_{10} & l_{20} & l_{30} \\ m_{10} & m_{20} & m_{30} \\ n_{10} & n_{20} & n_{30} \end{bmatrix} \begin{bmatrix} \dot{x} \\ \dot{y} \\ \dot{z} \end{bmatrix} - \begin{bmatrix} u_0 \\ v_0 \\ w_0 \end{bmatrix}$$

The body-axes accelerations are given by the same transformation :

$$\begin{bmatrix} \dot{u} \\ \dot{v} \\ \dot{w} \end{bmatrix} = \begin{bmatrix} l_{10} & l_{20} & l_{30} \\ m_{10} & m_{20} & m_{30} \\ n_{10} & n_{20} & n_{30} \end{bmatrix} \begin{bmatrix} \ddot{x} \\ \ddot{y} \\ \ddot{z} \end{bmatrix} - \begin{bmatrix} w_0 q - v_0 r \\ u_0 r - w_0 p \\ v_0 p - u_0 r \end{bmatrix} \dots\dots (7)$$

b) Yaw Rate and Acceleration

An expression relating yaw rate to the sideslip constraint can be developed from the second of equations (7) :

$$r = \frac{1}{u_0} (m_{10} \ddot{x} + m_{20} \ddot{y} + m_{30} \ddot{z} - \dot{v} + w_0 p)$$

and by differentiation :

$$\dot{r} = \frac{1}{u_0} (m_{10} \ddot{\ddot{x}} + m_{20} \ddot{\ddot{y}} + m_{30} \ddot{\ddot{z}} - \ddot{v} + w_0 \dot{p})$$

The fourth of the original linearised equations of motion is used for \dot{p} , i.e. from equation (1) :

$$\dot{p} = a_{41} u + a_{42} v + \dots\dots\dots + b_{44} \theta_{0tx}$$

where a_{41} , etc. are entries in the original system and control matrices. The sideslip angle is constrained as a function of time. Hence, the sideslip velocity is given by :

$$v = V \sin\beta \dots\dots (8)$$

The values of v and \dot{v} are found by differentiation of equation (8) :

$$\left. \begin{aligned} \dot{v} &= \dot{V} \sin\beta + V\dot{\beta} \cos\beta \\ \ddot{v} &= (\dot{\ddot{V}} - V\dot{\beta}^2) \sin\beta + (2\dot{V}\dot{\beta} + \ddot{\beta}V) \cos\beta \end{aligned} \right\} \dots\dots (9)$$

Using the relationships above to eliminate the state variables u, v, w, r and their rates of change gives a system with state and control matrices A_C and B_C as described above. The exact composition of A_C and B_C together with a detailed derivation is given in Reference 3.

4.3 The Oscillatory Nature of the Inverse Solution

From the analysis in the previous section, the modes of the modified, constrained system are found from the new "system matrix", A_C . Using the constrained system matrix A_C , it is possible to predict the oscillatory form of the solution. For the case of the SRR helicopter given above, calculation of the matrix A_C , and its associated eigenvalues for a trim flight velocity of 80 knots, gives the following two modes. The first is a divergent oscillation of period 0.69 seconds and time to double amplitude of 115 seconds. The second mode is a convergent oscillation of period 1.19 seconds and a time to half amplitude of 1.7 seconds. These periods show good correlation with those measured from the graphs on Figures 5 and 7 (0.7 and 1.0 seconds). A similar effect can be observed using different configurations and manoeuvres. These also explain the dependence on the time increment remarked upon earlier. A low order implicit method introduces an artificial damping, the effect of

which is reduced as the time increment becomes smaller and the numerical solution approaches the correct solution. It is clear from the numerical results obtained that the oscillations which become more noticeable as the time increment is reduced are those corresponding to the persistent, indeed unstable, oscillations with time to double amplitude of 115 seconds.

The above analysis gives an insight into another problem associated with the inverse solutions. It is noticeable from Figures 2, 5 and 7 that not all of the variables return to their commanded trim values. This can be explained by consideration of the flight path geometry at this point. At the exit, the polynomial representation of the manoeuvre is joined to a linear flight path. In the case of the hurdle-hop, there is only continuity up to the second derivative (i.e. the boundary condition at the exit is for zero acceleration). It is the discontinuity of the higher order derivatives which causes the apparent error at the exit. In an inverse solution, a discontinuity in the higher order flight path derivatives (i.e. a discontinuity in the "input signal") is analogous to a step input to a control variable in a conventional time response solution. The helicopter can therefore be expected to respond in a similar manner. The analysis given above predicts that the dynamics of a helicopter constrained to fly a fixed flight path are dominated by two oscillatory modes. The response of the helicopter, after encountering the discontinuity at the exit of the manoeuvre, will therefore be to oscillate towards the commanded trim state. This is most clearly demonstrated by the following example.

A pop-up manoeuvre can be considered as the first half of a hurdle-hop manoeuvre - a height gain either to avoid some obstacle or follow terrain. The flight path can be modelled using a fifth order polynomial with boundary conditions at the exit giving constant velocity at an altitude h . If a linear section is then joined to the exit of the pop-up, as in Figure 8, then the flight path derivatives above second order will be discontinuous. In effect there will be a step change in the input vector u_c . Due to the nature of the system, this step in the input signal should cause oscillations in the output variables (θ, ϕ, p, q) . This is clearly shown in Figure 9. This figure shows the time histories for the SRR configuration flying the extended pop-up manoeuvre, dimensions given in Figure 8, at a velocity of 120 knots. The pop-up section of the manoeuvre takes just under 5 seconds, after which all variables oscillate about their trim values. For a velocity 120 knots the eigenvalues of the modified system matrix give a divergent oscillation of period 0.75 with time to double amplitude of 80.9 seconds, and a convergent oscillation of period 1.22 and time to half amplitude of 1.03 seconds. From Figure 8, the periods of the oscillation are 1.05 seconds for (θ, q) and 0.72 seconds for (ϕ, p) . These values correspond to those predicted by the theory.

5. Conclusions

The oscillatory form of certain inverse solutions was initially thought to be caused by some sort of numerical inconsistency within the algorithm. However the analysis presented in this paper indicates that these oscillations are a direct consequence of the constraints imposed on the helicopter in terms of the precise definition of its velocities and accelerations. As the values of the original system and control matrices

A and B used in the above examples were calculated from HELISTAB, which is of proven validity, it follows that a real helicopter constrained in a similar manner, will respond in a similar way. The findings of this paper are therefore relevant to control system studies for helicopters which are guidance orientated, and to piloted conditions where a strict flight path is defined, for example in agility studies where circles or figures of eight are flown. This research will continue by examining flight data from such piloted exercises.

6. References

1. D.G. Thomson, "Mathematical Representation of Flight Paths Commonly Found in Helicopter Nap-of-the-Earth Flight", Glasgow University, Dept. of Aeronautics, Internal Report, In preparation.
2. D.G. Thomson, R. Bradley, "Recent Developments in the Calculation of Inverse Solutions of Helicopter Equations of Motion", **Conference Proceedings**, UK Simulation Council Conference, Sept. 1987.
3. D.G. Thomson, "Evaluation of Helicopter Agility Through Inverse Solution of the Helicopter Equations of Motion", **Ph.D. Thesis**, University of Glasgow, May 1987.
4. D.G. Thomson, "An Analytic Method of Quantifying Helicopter Agility", **Forum Proceedings**, 12th European Rotorcraft Forum, Paper No. 45, September 1986.
5. S. Houston, A.E. Caldwell, "A Computer Based Study of Helicopter Agility, Including the Influence of an Active Tailplane", **Forum Proceedings**, 10th European Rotorcraft Forum, Paper No. 70, Sept. 1984.
6. G.D. Padfield, "A Theoretical Model of Helicopter Flight Mechanics for Application to Piloted Simulation", **RAE TM 81048**, April 1981.

Acknowledgements

The authors would like to acknowledge the contributions of Dr. G.D. Padfield of the Royal Aircraft Establishment, Bedford to this work, particularly in relation to the HELISTAB model. This research was carried out as part of the Ministry of Defence Extra Mural Agreement 2048/39/XR/FS.

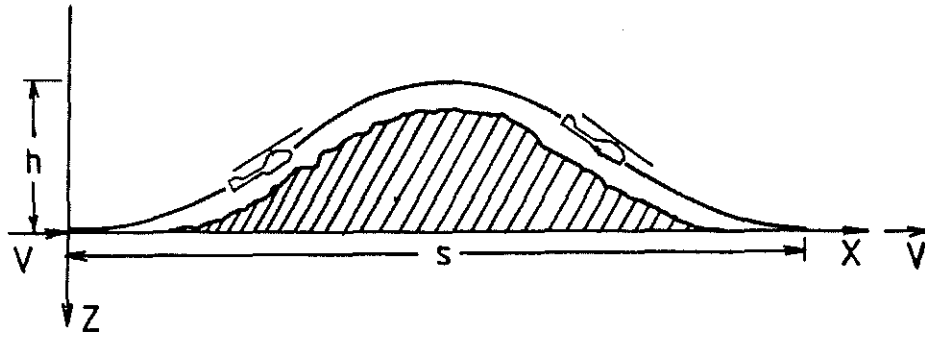


Figure 1 : The Hurdle-Hop Manoeuvre.

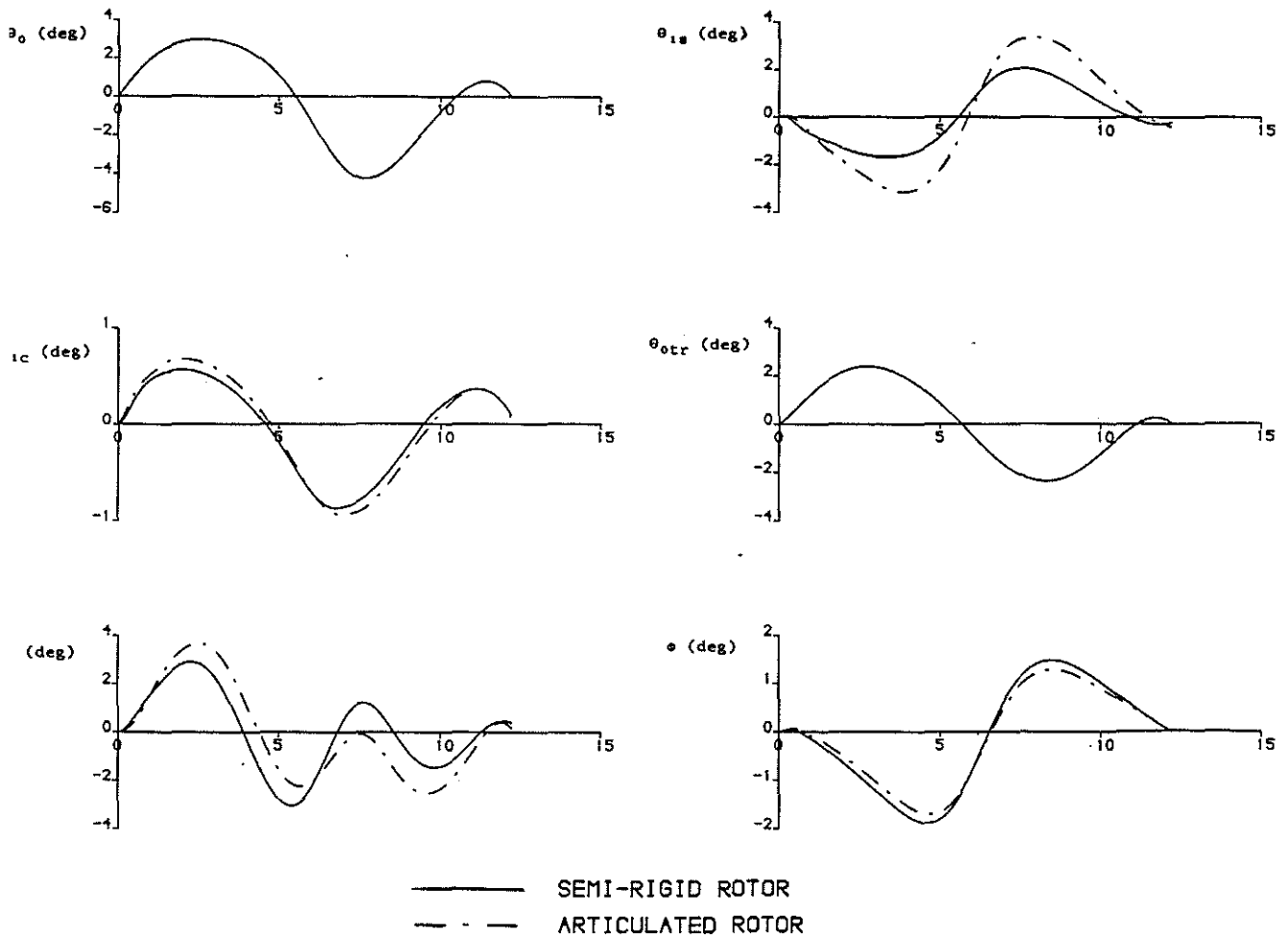


Figure 2 : Time Histories for Hurdle-Hop Manoeuvre of Dimensions
 $h = 25\text{m}$, $s = 500\text{m}$, Flown at a Constant Speed of 80 knots.

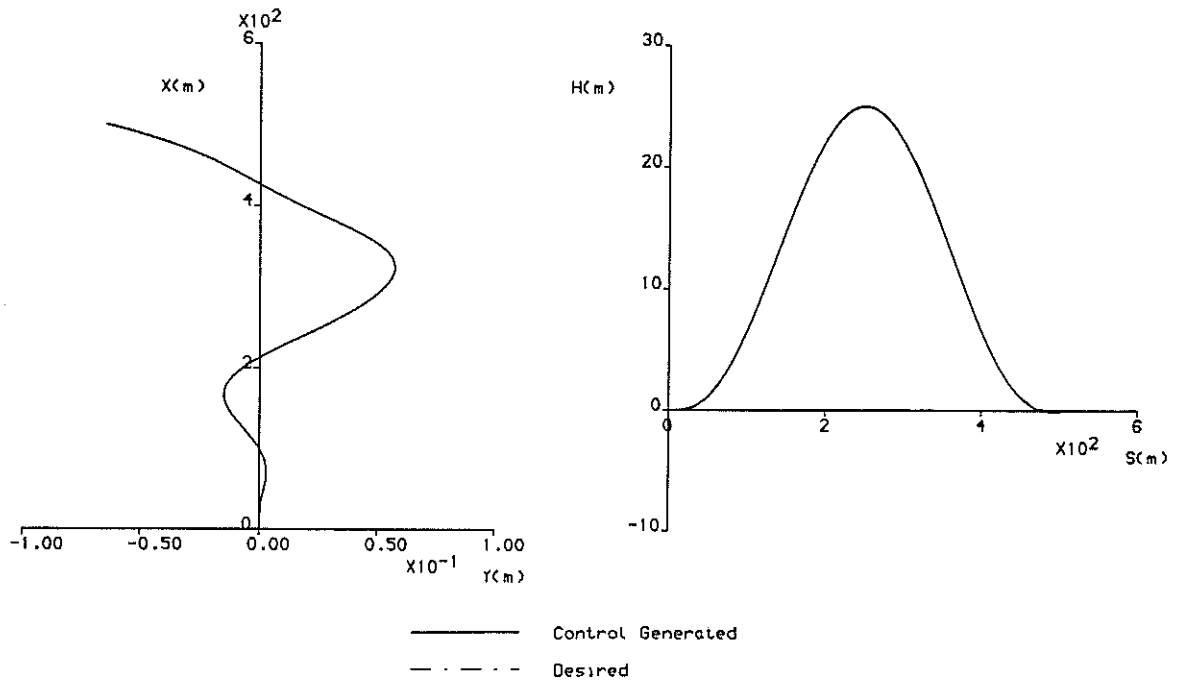


Figure 3 : Comparison of Inverse and Time Response Solutions for AR Configuration Flying the Hurdle-Hop Manoeuvre.

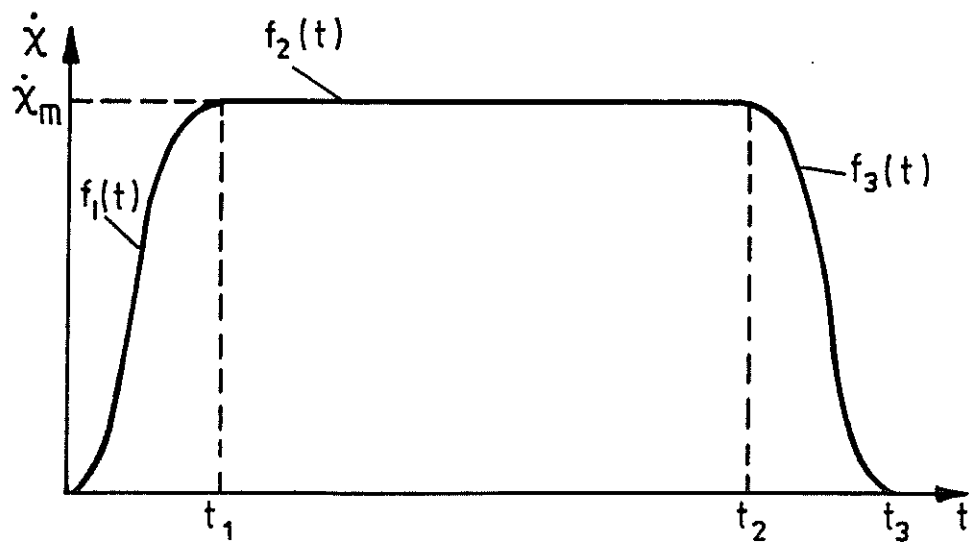


Figure 4 : Specification of Turn Rate for Constant Speed Level Turn.

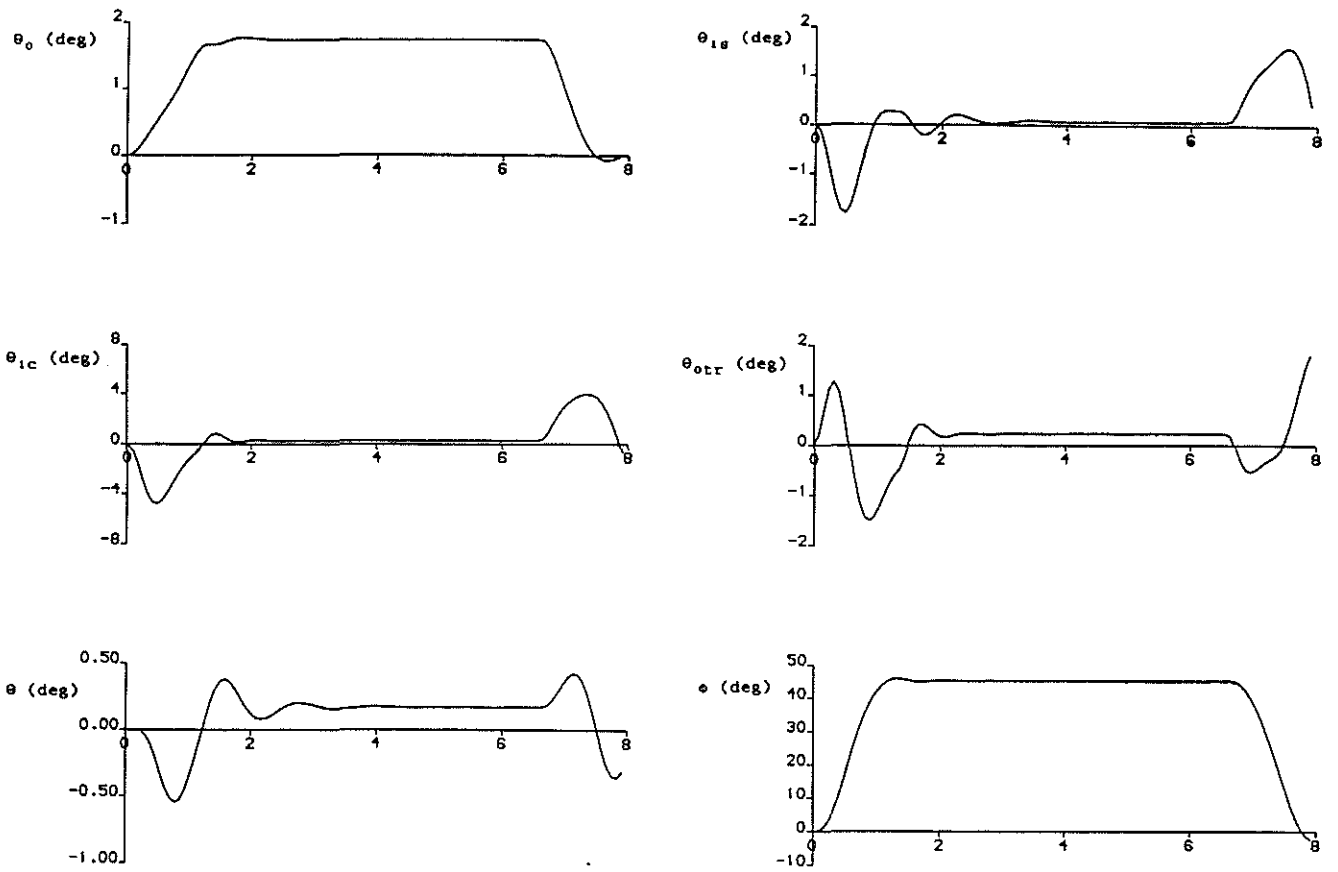


Figure 5 : Time Histories for a 200m Radius Turn Flown at 80 knots by the SRR Configuration ($\delta t = 0.08s$).

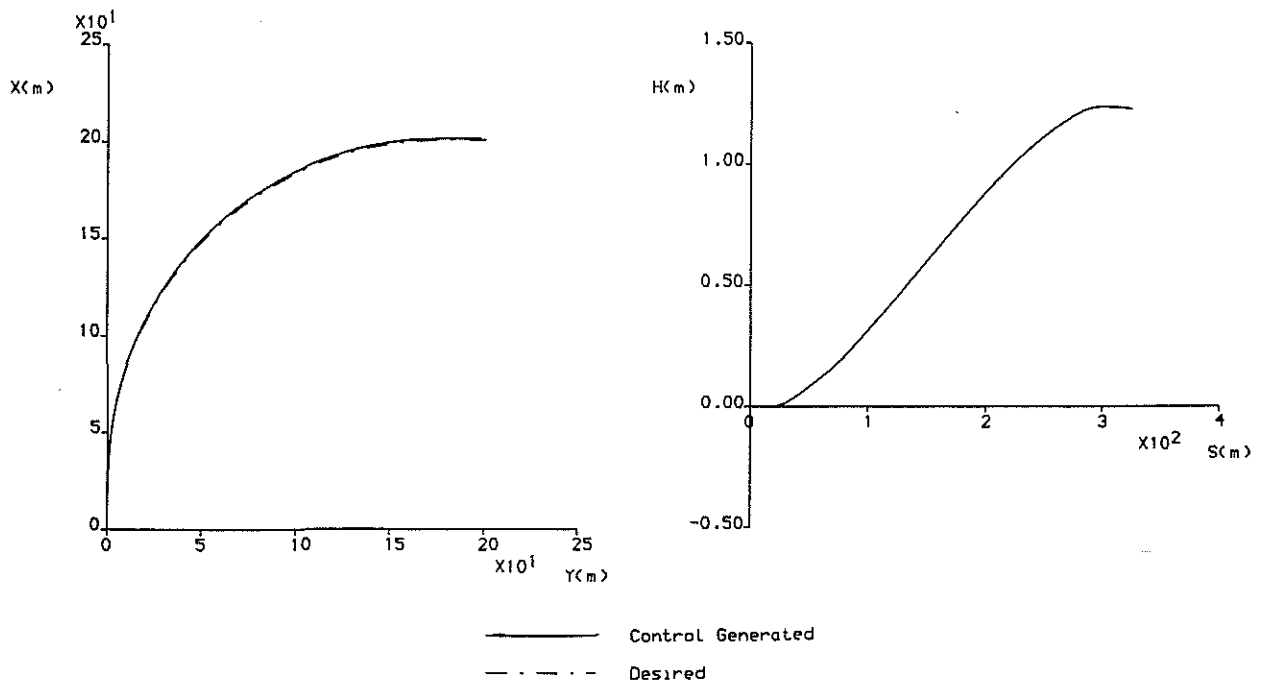


Figure 6 : Comparison of Inverse and Time Response Solutions for SRR Configuration Flying a Level Turn Manoeuvre.

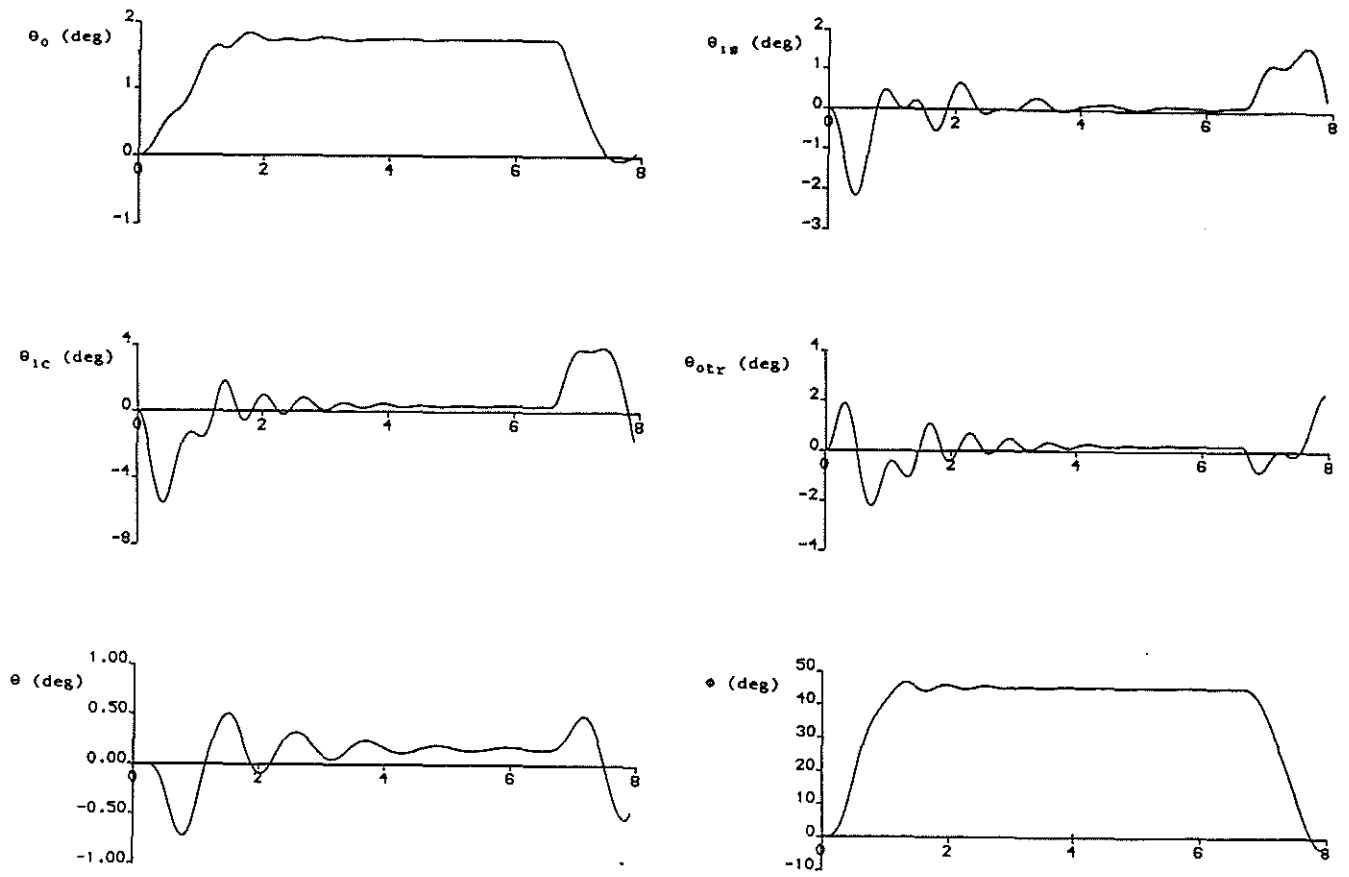


Figure 7 : Time Histories for a 200m Radius Turn Flown at 80 knots by the SRR Configuration ($\delta t = 0.02s$).

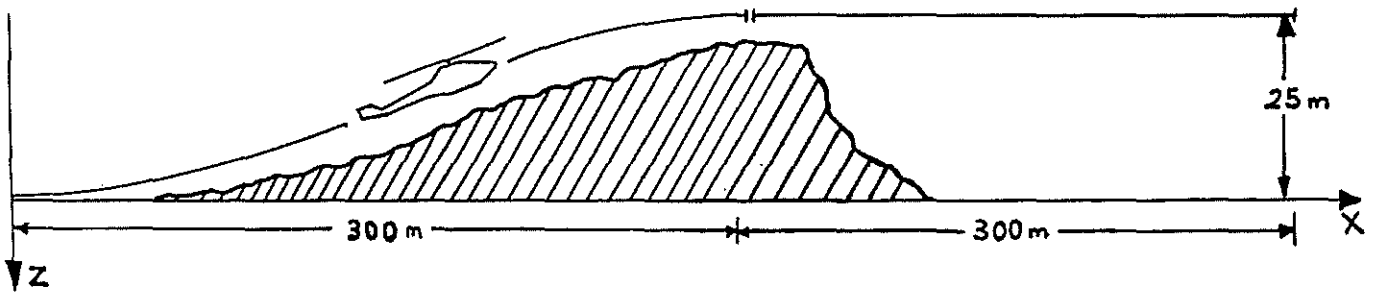


Figure 8 : Pop-up Manoeuvre With Linear Section at the Exit.

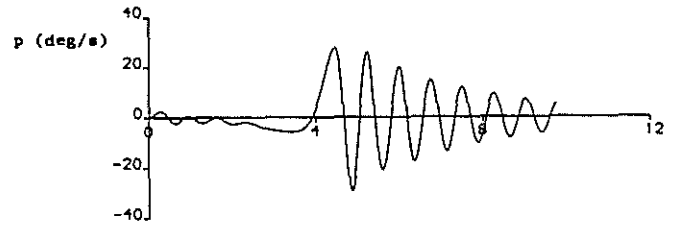
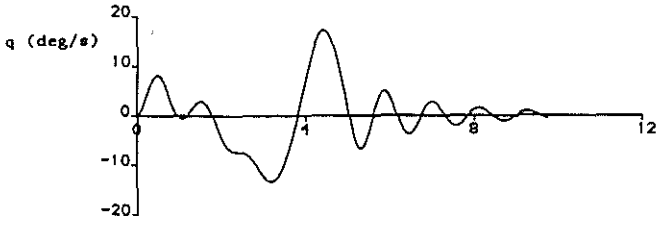
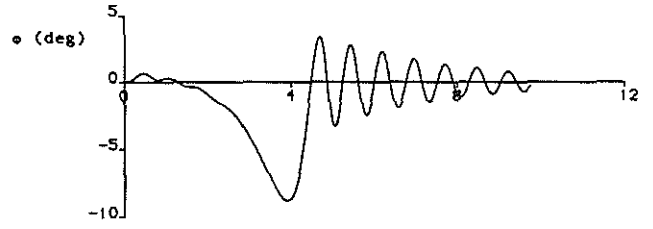
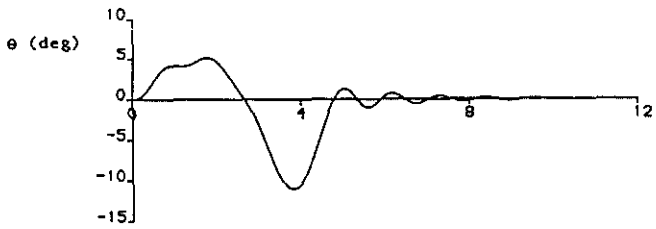


Figure 9 : Time Histories for SRR Configuration Flying an Extended Pop-up Manoeuvre at 120 knots.